



## Research articles

## Threshold behaviors of direct and Hall currents in topological spin-Hall effect

Andrei Zadorozhnyi, Yuri Dahnovsky\*

Department of Physics and Astronomy/3905, 1000 E. University Avenue, University of Wyoming, Laramie, WY 82071, United States of America

## ARTICLE INFO

## Keywords:

Skyrmions  
Topological spin Hall effect  
Boltzmann equation  
Spin transistor

## ABSTRACT

We study spin-dependent direct and Hall conductivities in the threshold region of Fermi energy,  $\epsilon_F = 2J$ , where  $J$  is the exchange integral between the conduction electron spins and the skyrmion spin texture. For  $\epsilon_F$  at the threshold value and above the spin-down electrons are allowed to exist. We find the two in the direct and four narrow peaks in the Hall conductivities for Fermi energies slightly below the threshold value. The found effects are dramatic because the electric current changes by approximately eight times in the narrow range of gate voltages ( $\sim 4$  meV). The values of the peaks strongly depend on skyrmion size. For small and very large skyrmion sizes the peak amplitudes are small compared to the conductivity absolute values. At the skyrmion radius  $a = 6$  nm and very light conduction electrons,  $m^* \sim 10^{-2}m_e$ , the extrema are the most pronounced. The temperature evolution reveals the strong smearing effect where the peak-wise behavior completely disappears at room temperatures. Spin transistor could be considered for possible applications where in the narrow region of gate voltage the sharp conductivity change occurs.

## 1. Introduction

Topological spin Hall effect (TSHE) can be determined because of the interaction of free electrons with topological magnetic textures, skyrmions. [1–14] The presence of spin-orbit coupling in such systems is crucial because this interaction is in charge of Dzyaloshinskii–Moriya interaction, and therefore, skyrmions. [1,10] To calculate the TSHE there are a few methodologies for weak conduction electron–skyrmion interaction [15,16], the tight-binding approximation, [17,18] the Berry phase [14,19] or the emergent field approach. [20–22] For the spin current calculations we employ the nonequilibrium Boltzmann equation. [1,23–33]

Two-dimensional free electron gas interacting with skyrmions in a ferromagnetic environment is a very interesting system to study a TSHE. In this work we study only electron–skyrmion scattering. The effect of electron–impurity scattering is not considered in order to elucidate pure nonlinear effects due to the electron–skyrmion interaction. For interaction between the localized magnetic moments (the skyrmions) and conduction electron spins we use the  $s$ - $d$  Hamiltonian: [34]

$$H = \left( \frac{\hbar^2 k^2}{2m} \hat{\mathbf{1}} - J \hat{\sigma}_z + J \hat{\mathbf{1}} \right) - J \delta \mathbf{n}(\mathbf{r}) \cdot \hat{\boldsymbol{\sigma}} = \hat{H}_0 + \hat{V}. \quad (1)$$

Here the first term represents the kinetic energy of conduction electrons, the second term describes the splitting due to the interaction between conduction electron and ferromagnetic moment, the third term is introduced for the convenience representing the constant energy

shift. The last term is exchange interaction between the conduction electrons and localized magnetic textures (skyrmions)  $\delta \mathbf{n}(\mathbf{r})$ .

In Refs. [32,33,35] the TSHE and spin Seebeck and Nernst effects [36] were studied in the case where the Fermi energy was large enough to fill up both lower and upper bands by the conduction electrons. The spin-up and spin-down bands are shown in Fig. 1. As soon as the Fermi energy is higher than the threshold value,  $\epsilon_F = 2J$ , we expect nonlinear behaviors in direct and Hall currents for both spin projections. However, the TSHE has not been investigated at  $\epsilon_F < 2J$  in the whole range of skyrmion sizes. As shown in Ref. [37] for large skyrmions the direct and Hall currents do not exhibit dramatic effects in the threshold region. However, for smaller and intermediate skyrmions and light conduction electrons the behavior of the TSHE could be dramatic. To fill up this gap, we study direct and Hall currents for the Fermi energies close to the threshold value, and anticipate dramatic behaviors in the direct and Hall currents for the spin-up components. The spin-down components of current are also investigated.

## 2. Calculation details

The direct and Hall conductivities for the spin-up and spin-down components are studied in the semiclassical approximation based on the Boltzmann equation (2). [38]

$$\frac{\partial f_0}{\partial \epsilon} e \mathbf{E} \cdot \mathbf{v}^s = \sum_{s'} \sum_{\mathbf{k}'} \left( W_{\mathbf{k}\mathbf{k}'}^{ss'} f_1^{s'}(\mathbf{k}') - W_{\mathbf{k}'\mathbf{k}}^{s's} f_1^s(\mathbf{k}) \right). \quad (2)$$

\* Corresponding author.

E-mail address: [yurid@uwyo.edu](mailto:yurid@uwyo.edu) (Y. Dahnovsky).<https://doi.org/10.1016/j.jmmm.2021.168492>

Received 28 June 2021; Received in revised form 4 August 2021; Accepted 28 August 2021

Available online 3 September 2021

0304-8853/© 2021 Elsevier B.V. All rights reserved.

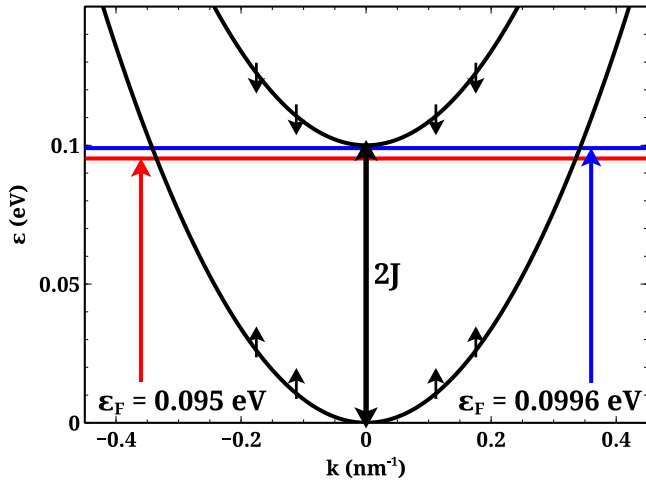


Fig. 1. Band structure for the spin-up (lower) and spin-down (upper) electrons. The splitting between the bands is equal to  $2J$ . The positions of  $\epsilon_F$  are shown by blue and red lines.

Here  $W_{kk'}^{ss'}$  is the probability rate from the electron state with wavevector  $k'$  and spin  $s'$  to the electron state with wavevector  $k$  and spin  $s$ .  $f_0$  denotes the equilibrium Fermi distribution function, and  $f_1^s(k)$  is a nonequilibrium distribution function correction. The applied electric field  $E$  is directed along the  $x$ -axis. For the scattering mechanism in Eq. (2) we only consider the electron-skyrmion scattering. Then the probability rate can be determined in terms of the transition matrix  $T_{kk'}^{ss'}$ : [39]

$$W_{kk'}^{ss'} = \frac{2\pi}{\hbar} n_{sk} |T_{kk'}^{ss'}|^2 \delta(\epsilon - \epsilon'). \quad (3)$$

Here  $n_{sk}$  is a skyrmion density. Electric currents and, therefore, conductivities are inversely proportional to  $n_{sk}$ . The transition matrix is determined from the Lippmann-Schwinger equation: [39]

$$\hat{T} = \hat{V} + \hat{V} \hat{G}_0 \hat{T}. \quad (4)$$

Here  $\hat{G}_0$  denotes a retarded free electron Green's function determined as follows: [40]

$$\hat{G}_0(\epsilon) = \lim_{\delta \rightarrow +0} [\epsilon \hat{1} - \hat{H}_0 + i\delta \hat{1}]^{-1} = \lim_{\delta \rightarrow +0} \left[ \left( \epsilon - \frac{\hbar^2 k^2}{2m} \right) \hat{1} + J \hat{\sigma}_z + i\delta \hat{1} \right]^{-1}. \quad (5)$$

The interaction potential energy operator,  $\hat{V}(\mathbf{r})$ , (see Eq. (1)) for a single skyrmion distribution is given by the matrix:

$$\hat{V}(\mathbf{r}) = -J \begin{pmatrix} \delta n_z(\mathbf{r}) & \delta n_x(\mathbf{r}) - i\delta n_y(\mathbf{r}) \\ \delta n_x(\mathbf{r}) + i\delta n_y(\mathbf{r}) & -\delta n_z(\mathbf{r}) \end{pmatrix}. \quad (6)$$

For the skyrmion magnetic moment distribution we choose the following analytic form: [41]

$$\delta n_z(r) = \begin{cases} 4 \left( \frac{r}{a} \right)^2 - 2, & r \leq a/2, \\ -4 \left( 1 - \frac{r}{a} \right)^2, & a/2 < r \leq a, \\ 0, & r > a, \end{cases} \quad (7)$$

$$\delta n_x(r) = \sqrt{1 - (\delta n_z(r) + 1)^2} \cos \alpha,$$

$$\delta n_y(r) = \sqrt{1 - (\delta n_z(r) + 1)^2} \sin \alpha,$$

where  $a$  is a skyrmion radius,  $r$  and  $\alpha$  are polar coordinates in a frame with the center of the skyrmion located at  $r = 0$ .

The spin-dependent direct and Hall components of the current (the conductivity) are found using the following equations: [38]

$$j_{x,y}^s = \sigma_{xx,yx} E_x = e \int v_{x,y} f_1^s(\mathbf{k}) d\mathbf{k}_x d\mathbf{k}_y. \quad (8)$$

Here  $v_{x,y}$  is an electron velocity, and  $f_1^s(\mathbf{k})$  is the nonequilibrium distribution function correction. It can be found from the Boltzmann equation (2).

The solutions of Lippmann-Schwinger (4) and Boltzmann (2) equations are found numerically writing the original codes. The computational details are given in Refs. [36,37]

### 3. Results and discussion

Inasmuch as we are interested in the behavior of the electric conductivity in the threshold region of  $\epsilon_F$ , we have calculated  $\epsilon_F$ -dependencies of the direct and Hall conductivities for the spin-up and spin-down components. The results of the calculations are presented in Figs. 2a–2d. The most dramatic behavior is observed for the spin-up components of the conductivity. Indeed, the spin-up direct conductivity (see Fig. 2a) exhibits the different dependencies for the various skyrmion sizes in the threshold region. For the smallest skyrmion size (the red line) the peaks are small with respect to the conductivity absolute value, while the sharp maximum and minimum are found for  $a = 6$  nm. At the larger skyrmion size (the black line) there is no extremum behavior. The Hall component,  $\sigma_{yx}^\uparrow$ , shown in Fig. 2b, exhibits some similarities and at the same time some differences compared to  $\sigma_{xx}^\uparrow$ . Indeed, the most pronounced effect is found for the skyrmion size  $a = 6$  nm. For smaller and larger skyrmion sizes the peak-wise dependencies are less pronounced. The main difference between the  $\sigma_{xx}^\uparrow$  and  $\sigma_{yx}^\uparrow$  conductivities is in the number of the extrema. For  $\sigma_{xx}^\uparrow$  in the narrow range of  $\epsilon_F$ , we observe one minimum and one maximum while for  $\sigma_{yx}^\uparrow$  there are two minima and two maxima at the Fermi energies that are slightly below the threshold value  $\epsilon_F = 2J$ . It is important to note that for small skyrmions ( $a = 1.5$  nm, 3.0 nm),  $\sigma_{xx}^\uparrow \gg |\sigma_{yx}^\uparrow|$ . Indeed, the forward scattering dominates because of the small size of the scatterers. For the larger skyrmion sizes ( $a = 6.0$  nm,  $a = 30$  nm)  $\sigma_{xx}^\uparrow$  and  $|\sigma_{yx}^\uparrow|$  are of the same order of magnitude. The spin-down direct and Hall conductivities are shown in Figs. 2c and 2d, respectively.  $\sigma_{xx}^\downarrow$  and  $|\sigma_{yx}^\downarrow|$  vanish for  $\epsilon_F < 2J$  because of the absence of spin-down carriers. If  $\epsilon_F > 2J$ , the sharp increase for the direct conductivity is found. The absolute values of  $\sigma_{yx}^\downarrow$  are also the growing functions. However, for the large skyrmion size ( $a = 30$  nm)  $\sigma_{yx} > 0$ , whereas  $\sigma_{yx}$  are negative for smaller sizes.

It is important to understand how the temperature smears the extrema shown in Fig. 2 where the sharpest dependencies in the conductivities occur at  $a = 6.0$  nm. For this size we present the direct (see Figs. 3a and 3c) and Hall (Figs. 3b and 3d) conductivities for the spin-up (see Figs. 3a and 3b) and spin-down (see Figs. 3c and 3d) conduction electrons for the three different temperatures. As expected, the sharpest behaviors of  $\sigma_{xx}^\uparrow$  and  $\sigma_{yx}^\uparrow$  occur at  $k_B T = 0$  eV. As temperature increases, the peaks are smeared and completely disappear at the room temperature ( $k_B T = 0.025$  eV). The absolute values of the spin-down direct and Hall conductivities are still the growing functions (as shown in Figs. 3c and 3d). At the room temperature, there is the nonvanishing spin-down conductivities for  $\epsilon_F < 2J$ . It happens because of the nonzero electron density above the threshold due to the temperature excitations.

In Figs. 4a and 4c we present the temperature evolution of the direct conductivity. As shown in Fig. 4a, the distinct maximum and minimum positions in  $\sigma_{xx}^\uparrow$  occur at temperatures  $k_B T < 0.005$  eV ( $T \approx 60$  K). At higher temperatures the peaks disappear. The temperature dependencies of the Hall conductivities are shown in Figs. 4b and 4d. The blue and red lines correspond to the peaks in Fig. 3b, while the green line denotes the minimum. The maxima and minimum converge (i.e., the extrema disappear) for  $k_B T = 0.002$  eV ( $T \approx 23$  K) that is two and a half times lower than that of the direct conductivity. For  $\sigma_{xx}^\downarrow$  and  $\sigma_{yx}^\downarrow$  (see Figs. 4c and 4d), the curves are close to each other in the whole region of temperatures because of the absence of the extrema (see Figs. 3c and 3d).

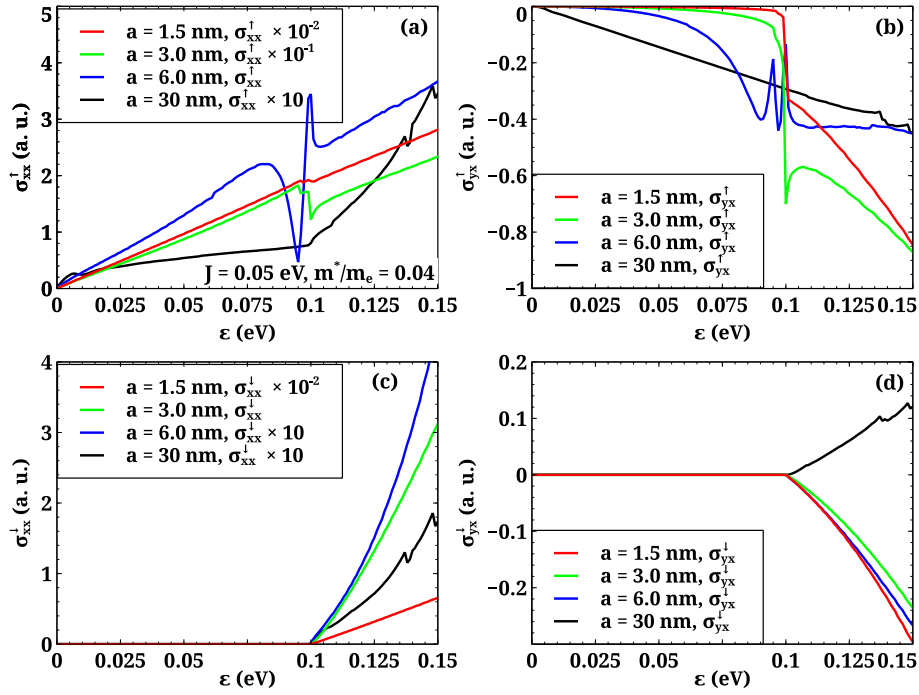


Fig. 2. Direct ((a) and (c)) and Hall ((b) and (d)) conductivities for spin-up ((a) and (b)) and spin-down ((c) and (d)) components for the various skyrmion sizes  $a = 1.5$  nm (the red line),  $a = 3.0$  nm (the green line),  $a = 6.0$  nm (the blue line), and  $a = 30$  nm (the black line) with respect to  $\epsilon_F$  at zero temperature.

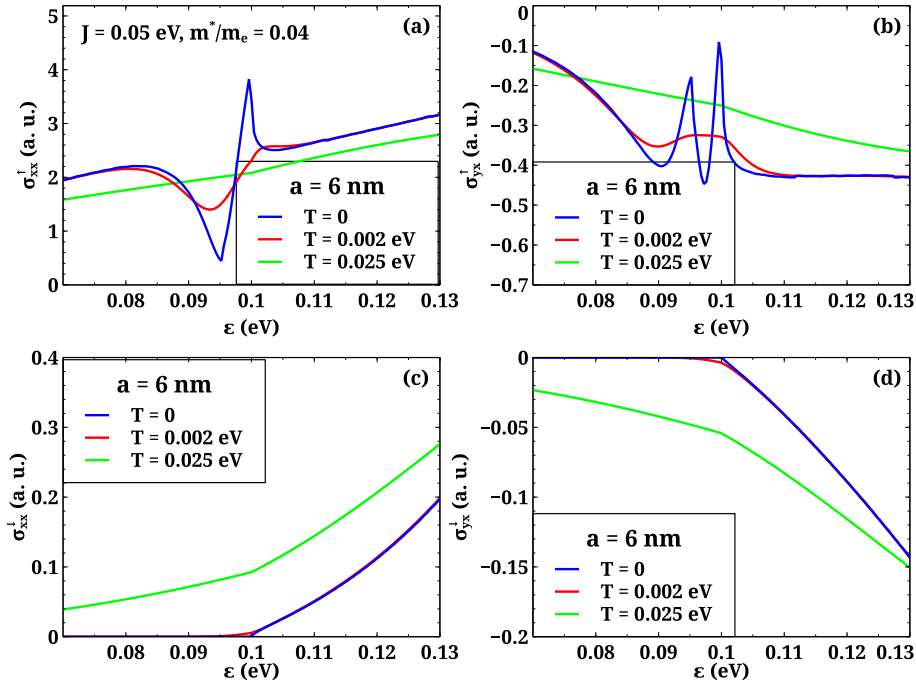


Fig. 3. Direct ((a) and (c)) and Hall ((b) and (d)) conductivities for spin-up ((a) and (b)) and spin-down ((c) and (d)) components for the various temperatures,  $k_B T = 0$  eV (the blue line),  $k_B T = 0.002$  eV (the red line), and  $k_B T = 0.025$  eV (the green line) with respect to  $\epsilon_F$  for the skyrmion size  $a = 6.0$  nm.

#### 4. Conclusions

In this research we study electron-skyrmion scattering where we disregard the interaction of conduction electrons with impurities in order to elucidate the dramatic effects due to the electron-skyrmion interaction. We have found the peak-wise behaviors in spin-up direct and Hall conductivities (see Figs. 2–3) with Fermi energy. Previously we studied the topological Hall effect in the whole range of  $\epsilon_F$  for large skyrmion sizes and heavy conduction electrons.[37] The calculations

for different skyrmion sizes and conduction electron masses reveal that the most dramatic behavior occurs for  $a = 6.0$  nm. For this skyrmion size the spin-up direct conductivity,  $\sigma_{xx}^\uparrow$ , exhibits one minimum and one maximum below the threshold value  $\epsilon_F = 2J$ . The spin-up Hall conductivity,  $\sigma_{yx}^\uparrow$ , has two minima and two maxima for  $\epsilon_F < 2J$ . The temperature smearing of these extrema for the spin-up direct and Hall conductivities takes place. We have found that the most pronounced effect occurs at lower temperatures, while the peak-wise behavior disappears at the room temperature as shown in Figs. 3a and 3b. For

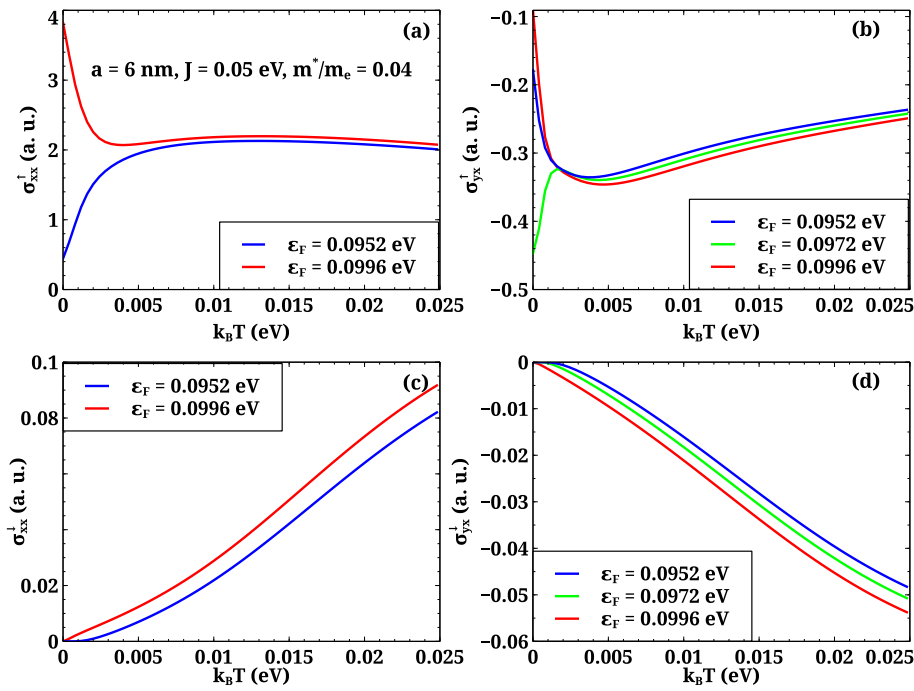


Fig. 4. Temperature evolution of the direct conductivity ((a) and (c)) at  $\epsilon_F = 0.0952$  eV (the blue line) and  $\epsilon_F = 0.0952$  eV (the red line), the minimum and maximum positions in Fig. 3a, and Hall ((b) and (d)) conductivities at  $\epsilon_F = 0.0952$  eV (the blue line),  $\epsilon_F = 0.0972$  eV (the green line),  $\epsilon_F = 0.0952$  eV (the red line), the minimum and maxima positions in Fig. 3b, for the spin-up ((a), (b)) and the spin-down ((c), (d)) components with respect to temperature. The skyrmion size is  $a = 6.0$  nm.

the spin-down conductivities (Figs. 3c and 3d), the nonvanishing value of the conductivity takes place for  $\epsilon_F$  below the threshold value. The peak-wise structure disappears with temperature in the spin-up direct conductivity at  $k_B T > 0.005$  eV (see Fig. 4a). For the spin-up Hall conductivity the peak-wise behavior disappears for  $k_B T > 0.002$  eV that is two and a half times lower than that of the direct conductivity.

The threshold effects could be applied to spin transistors where the amplitude of the spin-up current changes about one order of magnitude in the very narrow range of gate voltages, about 4 meV. For the practical use it is important to understand that the effects studied in this research disappears at  $T > 60$  K. The materials can be chosen in a broad range of exchange integrals,  $J$ . For example, the value of  $J = 0.3$  eV was experimentally found [42] and theoretically calculated [43] for 3D EuO crystals. For 2D materials a good candidate is  $\text{Cr}_2\text{Ge}_2\text{Te}_6$  where  $J = 0.02$  eV, [44] which is close to the value used in this work ( $J = 0.05$  eV). In addition, 2D  $\text{Cr}_2\text{Ge}_2\text{Te}_6$  material exhibits a skyrmion structure that is close to the physical model studied in this research. [45]

#### CRediT authorship contribution statement

**Andrei Zadorozhnyi:** Software, Visualization, Formal analysis, Investigation, Methodology, Writing. **Yuri Dahnovsky:** Conceptualization, Methodology, Formal analysis, Supervision, Project administration, Writing.

#### Declaration of competing interest

The authors declare that they have no known competing financial interests or personal relationships that could have appeared to influence the work reported in this paper.

#### Acknowledgments

This work was supported by a grant from the U S National Science Foundation (No. DMR-1710512) and the U S Department of Energy (No. DE-SC0020074) to the University of Wyoming.

#### References

- [1] N. Nagaosa, J. Sinova, S. Onoda, A.H. MacDonald, N.P. Ong, Anomalous Hall effect, *Rev. Modern Phys.* 82 (2010) 1539–1592, <http://dx.doi.org/10.1103/RevModPhys.82.1539>.
- [2] M. Lee, W. Kang, Y. Onose, Y. Tokura, N.P. Ong, Unusual Hall effect anomaly in MnSi under pressure, *Phys. Rev. Lett.* 102 (2009) 186601, <http://dx.doi.org/10.1103/PhysRevLett.102.186601>.
- [3] A. Neubauer, C. Pfleiderer, B. Binz, A. Rosch, R. Ritz, P.G. Niklowitz, P. Böni, Topological Hall effect in the A phase of MnSi, *Phys. Rev. Lett.* 102 (2009) 186602, <http://dx.doi.org/10.1103/PhysRevLett.102.186602>.
- [4] Y. Machida, S. Nakatsuji, Y. Maeno, T. Tayama, T. Sakakibara, S. Onoda, Unconventional anomalous Hall effect enhanced by a noncoplanar spin texture in the frustrated Kondo lattice  $\text{Pr}_2\text{Ir}_2\text{O}_7$ , *Phys. Rev. Lett.* 98 (2007) 057203, <http://dx.doi.org/10.1103/PhysRevLett.98.057203>.
- [5] C. Sürgers, G. Fischer, P. Winkel, H.V. Löhneysen, Large topological Hall effect in the non-collinear phase of an antiferromagnet, *Nat. Commun.* 5 (1) (2014) 3400, <http://dx.doi.org/10.1038/ncomms4400>.
- [6] B.G. Ueland, C.F. Miclea, Y. Kato, O. Ayala-Valenzuela, R.D. McDonald, R. Okazaki, P.H. Tobash, M.A. Torrez, F. Ronning, R. Movshovich, Z. Fisk, E.D. Bauer, I. Martin, J.D. Thompson, Controllable chirality-induced geometrical Hall effect in a frustrated highly correlated metal, *Nat. Commun.* 3 (1) (2012) 1067, <http://dx.doi.org/10.1038/ncomms2075>.
- [7] F.W. Fabris, P. Pureur, J. Schaf, V.N. Vieira, I.A. Campbell, Chiral anomalous Hall effect in reentrant AuFe alloys, *Phys. Rev. B* 74 (2006) 214201, <http://dx.doi.org/10.1103/PhysRevB.74.214201>.
- [8] Y. Ohuchi, Y. Kozuka, M. Uchida, K. Ueno, A. Tsukazaki, M. Kawasaki, Topological Hall effect in thin films of the Heisenberg ferromagnet EuO, *Phys. Rev. B* 91 (2015) 245115, <http://dx.doi.org/10.1103/PhysRevB.91.245115>.
- [9] L.N. Oveshnikov, V.A. Kulbachinskii, A.B. Davydov, B.A. Aronzon, I.V. Rozhansky, N.S. Averkiev, K.I. Kugel, V. Tripathi, Berry phase mechanism of the anomalous Hall effect in a disordered two-dimensional magnetic semiconductor structure, *Sci. Rep.* 5 (2015) 17158, <http://dx.doi.org/10.1038/srep17158>.
- [10] N. Nagaosa, Y. Tokura, Topological properties and dynamics of magnetic skyrmions, *Nat. Nanotechnol.* 8 (12) (2013) 899–911, <http://dx.doi.org/10.1038/nnano.2013.243>.
- [11] N. Kanazawa, M. Kubota, A. Tsukazaki, Y. Kozuka, K.S. Takahashi, M. Kawasaki, M. Ichikawa, F. Kagawa, Y. Tokura, Discretized topological Hall effect emerging from skyrmions in constricted geometry, *Phys. Rev. B* 91 (2015) 041122, <http://dx.doi.org/10.1103/PhysRevB.91.041122>.
- [12] S. Mühlbauer, B. Binz, F. Jonietz, C. Pfleiderer, A. Rosch, A. Neubauer, R. Georgii, P. Böni, Skyrmion lattice in a chiral magnet, *Science* 323 (5916) (2009) 915–919, <http://dx.doi.org/10.1126/science.1166767>.

- [13] Y. Li, N. Kanazawa, X.Z. Yu, A. Tsukazaki, M. Kawasaki, M. Ichikawa, X.F. Jin, F. Kagawa, Y. Tokura, Robust formation of skyrmions and topological Hall effect anomaly in epitaxial thin films of MnSi, *Phys. Rev. Lett.* 110 (2013) 117202, <http://dx.doi.org/10.1103/PhysRevLett.110.117202>.
- [14] P. Bruno, V.K. Dugaev, M. Taillefer, Topological Hall effect and Berry phase in magnetic nanostructures, *Phys. Rev. Lett.* 93 (2004) 096806, <http://dx.doi.org/10.1103/PhysRevLett.93.096806>.
- [15] M. Onoda, G. Tatara, N. Nagaosa, Anomalous Hall effect and skyrmion number in real and momentum spaces, *J. Phys. Soc. Japan* 73 (10) (2004) 2624–2627, <http://dx.doi.org/10.1143/JPSJ.73.2624>.
- [16] G. Tatara, H. Kawamura, Chirality-driven anomalous Hall effect in weak coupling regime, *J. Phys. Soc. Japan* 71 (11) (2002) 2613–2616, <http://dx.doi.org/10.1143/JPSJ.71.2613>.
- [17] J.-i. Ohe, T. Ohtsuki, B. Kramer, Mesoscopic Hall effect driven by chiral spin order, *Phys. Rev. B* 75 (2007) 245313, <http://dx.doi.org/10.1103/PhysRevB.75.245313>.
- [18] P.B. Ndiaye, C.A. Akosa, A. Manchon, Topological Hall and spin Hall effects in disordered skyrmionic textures, *Phys. Rev. B* 95 (2017) 064426, <http://dx.doi.org/10.1103/PhysRevB.95.064426>.
- [19] J. Ye, Y.B. Kim, A.J. Millis, B.I. Shraiman, P. Majumdar, Z. Tešanović, Berry phase theory of the anomalous Hall effect: Application to colossal magnetoresistance manganites, *Phys. Rev. Lett.* 83 (1999) 3737–3740, <http://dx.doi.org/10.1103/PhysRevLett.83.3737>.
- [20] N. Nagaosa, Y. Tokura, Emergent electromagnetism in solids, *Phys. Scr.* T146 (2012) 014020, <http://dx.doi.org/10.1088/0031-8949/2012/t146/014020>.
- [21] T. Fujita, M.B.A. Jalil, S.G. Tan, S. Murakami, Gauge fields in spintronics, *J. Appl. Phys.* 110 (12) (2011) 121301, <http://dx.doi.org/10.1063/1.3665219>.
- [22] G. Tatara, N. Nakabayashi, Emergent spin electromagnetism induced by magnetization textures in the presence of spin-orbit interaction (invited), *J. Appl. Phys.* 115 (2014) <http://dx.doi.org/10.1063/1.4870919>.
- [23] J.M. Luttinger, W. Kohn, Motion of electrons and holes in perturbed periodic fields, *Phys. Rev.* 97 (1955) 869–883, <http://dx.doi.org/10.1103/PhysRev.97.869>.
- [24] J.M. Luttinger, Theory of the Hall effect in ferromagnetic substances, *Phys. Rev.* 112 (1958) 739–751, <http://dx.doi.org/10.1103/PhysRev.112.739>.
- [25] J. Smit, The spontaneous Hall effect in ferromagnetics I, *Physica* 21 (6) (1955) 877–887, [http://dx.doi.org/10.1016/S0031-8914\(55\)92596-9](http://dx.doi.org/10.1016/S0031-8914(55)92596-9).
- [26] L. Berger, Side-jump mechanism for the Hall effect of ferromagnets, *Phys. Rev. B* 2 (1970) 4559–4566, <http://dx.doi.org/10.1103/PhysRevB.2.4559>.
- [27] T. Jungwirth, Q. Niu, A.H. MacDonald, Anomalous Hall effect in ferromagnetic semiconductors, *Phys. Rev. Lett.* 88 (2002) 207208, <http://dx.doi.org/10.1103/PhysRevLett.88.207208>.
- [28] N.A. Sinitsyn, Semiclassical theories of the anomalous Hall effect, *J. Phys. Condens. Matter* 20 (2) (2007) 023201, <http://dx.doi.org/10.1088/0953-8984/20/02/023201>.
- [29] N.A. Sinitsyn, A.H. MacDonald, T. Jungwirth, V.K. Dugaev, J. Sinova, Anomalous Hall effect in a two-dimensional Dirac band: The link between the Kubo–Streda formula and the semiclassical Boltzmann equation approach, *Phys. Rev. B* 75 (2007) 045315, <http://dx.doi.org/10.1103/PhysRevB.75.045315>.
- [30] N.A. Sinitsyn, Q. Niu, A.H. MacDonald, Coordinate shift in the semiclassical Boltzmann equation and the anomalous Hall effect, *Phys. Rev. B* 73 (2006) 075318, <http://dx.doi.org/10.1103/PhysRevB.73.075318>.
- [31] N.A. Sinitsyn, Q. Niu, J. Sinova, K. Nomura, Disorder effects in the anomalous Hall effect induced by Berry curvature, *Phys. Rev. B* 72 (2005) 045346, <http://dx.doi.org/10.1103/PhysRevB.72.045346>.
- [32] K.S. Denisov, I.V. Rozhansky, N.S. Averkiev, E. Lähderanta, Electron scattering on a magnetic skyrmion in the nonadiabatic approximation, *Phys. Rev. Lett.* 117 (2016) 027202, <http://dx.doi.org/10.1103/PhysRevLett.117.027202>.
- [33] K.S. Denisov, I.V. Rozhansky, N.S. Averkiev, E. Lähderanta, General theory of the topological Hall effect in systems with chiral spin textures, *Phys. Rev. B* 98 (2018) 195439, <http://dx.doi.org/10.1103/PhysRevB.98.195439>.
- [34] A.C. Hewson, The Kondo Problem to Heavy Fermions, in: *Cambridge Studies in Magnetism*, Cambridge University Press, 1993, <http://dx.doi.org/10.1017/CBO9780511470752>.
- [35] A. Zadorozhnyi, Y. Dahnovsky, Spin filtering and spin separation in 2D materials by topological spin Hall effect, *J. Phys. Condens. Matter* 32 (40) (2020) 405803, <http://dx.doi.org/10.1088/1361-648x/ab926c>.
- [36] A. Zadorozhnyi, Y. Dahnovsky, Spin-dependent seebeck and nernst effects in an ideal skyrmion gas, *J. Magn. Magn. Mater.* 518 (2021) 167367, <http://dx.doi.org/10.1016/j.jmmm.2020.167367>.
- [37] A. Zadorozhnyi, Y. Dahnovsky, Temperature effects in spin-dependent Hall currents in an ideal skyrmion gas, *Phys. Rev. B* 103 (2021) 184418, <http://dx.doi.org/10.1103/PhysRevB.103.184418>.
- [38] A. Anselm, *Introduction to Semiconductor Theory*, Mir, Moscow, 1981.
- [39] J.R. Taylor, *Scattering Theory: The Quantum Theory on Nonrelativistic Collisions*, Wiley, New York, 1972.
- [40] A.L. Fetter, J.D. Walecka, *Quantum Theory of Many-Particle Systems*, Dover Publications, New York, 2003.
- [41] S.S. Pershoguba, S. Nakosai, A.V. Balatsky, Skyrmion-induced bound states in a superconductor, *Phys. Rev. B* 94 (2016) 064513, <http://dx.doi.org/10.1103/PhysRevB.94.064513>.
- [42] P.G. Steeneken, L.H. Tjeng, I. Elfmov, G.A. Sawatzky, G. Ghiringhelli, N.B. Brookes, D.-J. Huang, Exchange splitting and charge carrier spin polarization in EuO, *Phys. Rev. Lett.* 88 (2002) 047201, <http://dx.doi.org/10.1103/PhysRevLett.88.047201>, URL <https://link.aps.org/doi/10.1103/PhysRevLett.88.047201>.
- [43] J. An, K. Belashchenko, Electronic structure and magnetic properties of Gd-doped and Eu-rich EuO, *Phys. Rev. B* 88 (2013) 054421, <http://dx.doi.org/10.1103/PhysRevB.88.054421>.
- [44] W.-n. Ren, K.-j. Jin, J.-s. Wang, C. Ge, E.-J. Guo, C. Ma, C. Wang, X. Xu, Tunable electronic structure and magnetic anisotropy in bilayer ferromagnetic semiconductor Cr<sub>2</sub>Ge<sub>2</sub>Te<sub>6</sub>, *Sci. Rep.* 11 (1) (2021) 2744, <http://dx.doi.org/10.1038/s41598-021-82394-y>.
- [45] M.-G. Han, J.A. Garlow, Y. Liu, H. Zhang, J. Li, D. DiMarzio, M.W. Knight, C. Petrovic, D. Jariwala, Y. Zhu, Topological magnetic-spin textures in two-dimensional van der Waals Cr<sub>2</sub>Ge<sub>2</sub>Te<sub>6</sub>, *Nano Lett.* 19 (11) (2019) 7859–7865, <http://dx.doi.org/10.1021/acs.nanolett.9b02849>.